Rayko Simura*, Tetsuo Taniuchi, Kazumasa Sugiyama and Tsuguo Fukuda

Textural and Optical Properties of Ce-Doped YAG/Al_2O_3 Melt Growth Composite Grown by Micro-Pulling-Down Method

DOI 10.1515/htmp-2016-0152
Received July 10, 2016; accepted December 16, 2016

Abstract: Ce-doped YAG/Al_2O_3 melt-growth composite (MGC) samples were grown by the micro-pulling-down (μ-PD) method, and their physical and chemical properties were investigated. The grown MGC samples exhibit fine-grained granophyric texture at the micron scale. Fluorescence spectra, excited by a blue laser diode, were recorded, and, in particular, the finely textured granophyric MGC sample doped with 0.1 at% Ce and prepared with a growth rate of 3 mm/min shows superior fluorescence properties without high-temperature deterioration of fluorescence intensity. The μ-PD method is demonstrated to be applicable for manufacturing finely textured MGC samples with improved luminous efficiency as phosphors for white LEDs.

Keywords: melt-growth composites, Ce fluorescence, white LED, phosphors

PACS® (2010). 78.55.Hx, 81.30.-t, 81.10.Fq

Introduction

Directionally solidified eutectic-melt-growth composites have complicated but homogenous, fine, microscopic, multi-phase texture with reduced interphase spacing [1]. The materials are sometimes simply called MGCs (melt-growth composites). The MGC composed of yttrium aluminum garnet ($Y_3Al_5O_{12}$; YAG) and corundum (Al_2O_3) with granophyric texture is one of the most well known MGC materials. MGCs have physically and chemically stable features up to near the melting temperature, and they are expected to have applications as high-strength structural materials [2].

Recently, Ce-doped YAG/Al_2O_3 MGC was proposed as a superior phosphor material for high-power, white-light-emitting diodes (LED) excited by blue LEDs or laser diodes (LD) [3]. The important factors for light-emitting efficiency are distribution and/or grain size of the phosphor phase and interface conditions at grain boundaries, such as adhesion degree, which affects the fluorescence damping. These factors encourage the advancement of manufacturing technology for Ce-doped YAG/Al_2O_3 MGC with reduced or cohesive interphase spacing. The size of the fluorescent YAG phase with Ce in the granophyric texture can be controlled by growth rate. From this viewpoint, the micro-pulling-down (μ-PD) method is a promising crystal growth technique for MGC that allows us to optimize the growth rate within a relatively high-speed range (up to about 5 mm/min) [4, 5].

This paper presents the results of the first attempt to produce Ce-doped YAG/Al_2O_3 MGC by the μ-PD method. MGC rod samples with various concentrations of Ce have been systematically grown by the μ-PD method and characterized by textural observation, fluorescence spectra, and fluorescence intensity.

Materials and methods

Growth conditions

The μ-PD method was used to grow Ce-doped YAG/Al_2O_3 MGCs with nominal compositions of $(Ce_xY_{1-x})_3Al_5O_{12}/Al_2O_3$ (x = 0.001,0.005, and 0.01). Raw powder mixtures were prepared with the chemicals Al_2O_3 (4N, Kojundo kagaku), Y_2O_3 (4N, Kojundo kagaku), and CeO_2 (4N, Kojundo kagaku). Preliminary sintering of the mixtures was done at 1,400 °C for 24 h in alumina crucibles. Then, the sintered powders were set into an Ir crucible having the square die (5 mm x 5 mm) with a capillary hole of about 300 μm in diameter on the bottom of the crucible. The Ir crucible was heated by a radio-frequency induction device under Ar

***Corresponding author: Rayko Simura,** Institute for Materials Research, Tohoku University, Katahira 2-1-1, Aobaku, Sendai, Miyagi 980–8577, Japan, E-mail: ray@imr.tohoku.ac.jp
Tetsuo Taniuchi, Frontier Research Institute for Interdisciplinary Science, Tohoku University, Aramakiaza Aoba 6–3, Aobaku, Sendai 980–8578, Japan
Kazumasa Sugiyama, Institute for Materials Research, Tohoku University, Katahira 2-1-1, Aobaku, Sendai, Miyagi 980–8577, Japan
Tsuguo Fukuda, Fukuda Crystal Laboratory Co. Ltd., Minami-Yoshinari 6-6-3, Aobaku, Sendai, Miyagi 989–3204, Japan

atmosphere. After the starting materials in the crucible were melted, the melt came out through the hole and was subsequently pulled down using a *c*-axis Al_2O_3 seed prepared by the Czochralski method. In the present study, the pulling rate was set at 1, 3, or 5 mm/min. Typical weight and length of the grown sample were ~11 g and 10 cm. Obtained samples were sliced perpendicular to the growth direction for the characterization measurements. Some sliced samples were crushed in a mortar, and the obtained powder was used for phase confirmation by powder X-ray diffraction (XRD: Rigaku Ultima III) using Cu*Kα* radiation.

Textural observations and chemical composition

Sliced samples were subjected to mirror polishing treatment before observation, and the surface was coated with carbon using a vapor deposition technique. Microstructures of the samples were observed by means of back-scattered electron imaging (BEI) with a scanning electron microscope system (SEM; Hitachi S-3400N). The Ce-distribution mapping (Ce-Map) was carried out by electron micro-probe analysis (EPMA) using stage scanning and X-ray wavelength-dispersive spectroscopy (WDS) (JEOL JXA-8530F). The obtained data were examined using the ImageJ (v1.48) software package [6]. The crystal orientations in the textures were examined using electron backscatter diffraction patterns (EBSD; Detector: TSL solutions, Software: OIM Data Collection and Analysis). Sliced samples 1 mm thick were used for measurement of bulk Ce content by inductively-coupled plasma mass spectrometry (ICP-MS; Thermo Fisher Scientific ELEMENT2).

Optical measurements

For optical measurements, 0.1 and 0.5 at% Ce-doped MGC samples were used. Fluorescence spectra excited by a 445 nm laser diode operated at 300 mW were obtained using Ocean Optics HR4C1751. The fluorescence intensity of yellow and blue components excited by the same equipment was measured using an optical power meter with appropriate filters. Temperature dependence of fluorescence intensity was analyzed at intervals of 25 K from room temperature (RT; 25 °C) to 200 °C.

Results and discussion

Growth results

The grown MGC samples were opaque and yellowish in color. The XRD patterns of the crushed powder samples showed that they were composed of YAG (garnet) and Al_2O_3 (corundum) phases. Figure 1 shows the appearance of MGC samples with 0.5 at% Ce prepared using different growth rates. The MGC samples solidified with growth rates of 1 and 3 mm/min took the forms of tetragonal rods with approximate dimensions of 5 mm × 5 mm × 100 mm. The sample grown at 1 mm/min (Figure 1(a)) showed a square cross section with sharp corners, but that grown at 3 mm/min (Figure 1(b)) showed a square cross section with rounded corners. On the other hand, the sample grown at 5 mm/min exhibited a round cross-section, and the cross-section diameter varied irregularly along the length of the rod as shown in Figure 1(c). The resulting length of the

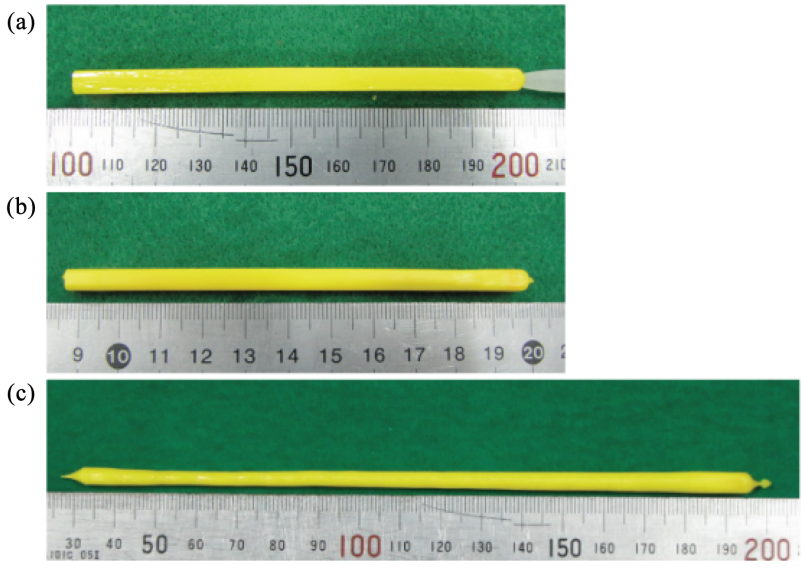

Figure 1: Photographs of typical grown samples. As-grown YAG/Al_2O_3 MGC samples doped with 0.5 at% Ce and grown by the μ-PD method with growth rates of 1 (a), 3 (b), and 5 mm/min (c).

5 mm/min sample reached 170 mm. This behavior of the sample shape associated with the growth rate was also observed for the samples with 0.1 at% and 1 at% Ce, suggesting that the whole shape can be controlled by changing the growth rate. The balance between the melt supply from the capillary hole of the crucible and the melt consumption at the melt/crystal interface appeared to be lost at high growth rates such as 5 mm/min.

Textures and composition

The grown samples had microscopic granophyric texture with YAG and Al_2O_3 phases, where YAG and Al_2O_3 can be easily identified as white and black regions in BEI, respectively (Figure 2(a)–(c)). The shape of the YAG-phase regions is reminiscent of hieroglyphics, and YAG regions are sometimes three-dimensionally connected with each other. The size of the YAG "glyphs" in the prepared Ce-doped samples showed a bimodal distribution, although the undoped YAG/Al_2O_3 MGCs do not exhibit texture with a bimodal size distribution for the YAG regions [4]. The areas composed of fine-sized "glyphs" (F areas) form "island"-like shapes and comprise the majority of the sample. The F area is surrounded by a belt-like area composed of coarser-sized "glyphs" (C area) as shown in Figure 2(a)–(c). As listed in Table 1, the "glyph" sizes in these two areas become smaller as the growth rates become larger. The same behavior in which the size decreases as the growth rate increases was observed for all the samples irrespective of the initial Ce contents. The observed "glyph" sizes of the μ-PD samples were smaller than that of the Ce-doped MGC samples grown by the ordinary Bridgeman (Bz) method [3]. The typical YAG "glyph" size for the sample grown by the Bz method

Table 1: Summary of typical YAG "glyph" size in F and C areas and the presence or absence of S areas in the grown samples.

Growth rate	1 mm/min	3 mm/min	5 mm/min
Glyph size in area F	~1.5 μm × ~5 μm	~1 μm × ~5 μm	~0.8 μm × ~4 μm
Glyph size in area C	~5 μm × ~30 μm	~4 μm × ~15 μm	~3 μm × ~10 μm
area S	Absent	Absent	Present

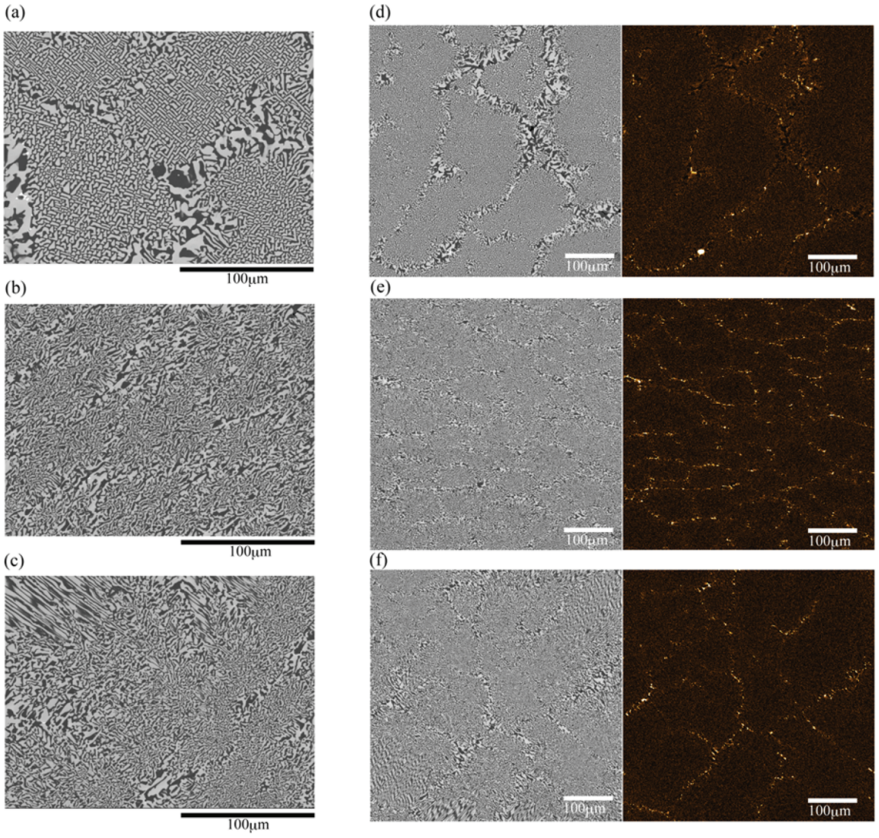

Figure 2: BEI data and Ce map of the grown samples. Backscatter images of YAG/Al_2O_3 MGC samples with 0.5 at% Ce grown at 1 (a), 3 (b), and 5 mm/min (c). Image pairs (d)–(f) are backscatter images (left) and the corresponding Ce maps (right) of the same areas. Ce content increases as color changes from black to white via orange. Coarse- and fine-grained regions (C and F areas, respectively) are present in all samples. The striped region (S area) is observed only in (c) and (f). C areas corresponds to the Ce-enriched regions.

(~75 μm × ~175 μm [3]) was almost as same as the "island" size of the F area for the μ-PD-grown MGC.

In addition to the F and C areas, the 5 mm/min sample had an area showing a striped pattern (S area) near the margin of the sample (Figure 2(c)). The striped texture corresponds to the cross-section texture parallel to the growth direction for the MGC grown by μ-PD [4], suggesting local horizontal growth in the S area. This means the growth rate of 5 mm/min is too high for stable growth of MGC in the current thermal configuration of our μ-PD furnace.

As shown in Figure 2(d)–(f), the Ce maps indicate that there are belt-like regions having a phase with higher Ce content. In the Ce-rich "belt," the Ce-rich phases are mainly the YAG phase of the C area. In addition, small grains of CeO_2 were occasionally observed as small spots. The samples with 1.0 at% Ce had many CeO_2 small grains and were not suitable for optical measurements. Bulk Ce content measured by ICP-MS is listed in Table 2. The bulk distribution coefficient (Ce in MGC)/(Ce in melt), is ~0.6 on average, suggesting that the Ce entrainment in the bulk MGC is higher than that of Ce:YAG single crystal (~0.1 [7]). From EBSD measurements, the crystal direction of the Al_2O_3 phase for the 1 mm/min sample was found to be <001>along the growth direction, which was inherited from the seed direction, but those of the YAG phase were varied depending on each F area "island". The boundary of each area having the same crystal directions of YAG is located at the halfway line of the C area "belt."

We attribute the appearance of the above-mentioned MGC textures to a possible phase-diagram modification caused by the minor component (Ce). All the described phenomena can be explained as follows: (1) Crystallization starts from around the center of the F-area "island" toward the rim of the "island"; (2) The residual melt is enriched with Ce and gathers at the "belt" region located at the marginal region of the "island"; (3) Then the melt crystallizes and forms the "belt"-like C areas having coarser YAG phase with higher Ce content and small amount of CeO_2 grains. Considering these processes, we anticipate that improvement of the textural homogeneity of Ce-doped MGC grown by μ-PD is possible by adjusting the chemical composition of the starting material and/or by optimizing the crucible shape and thermal conditions around the crucible in order to control the flow of the residual melt.

Optical measurements

Fluorescence spectra for the MGC samples grown at 3 mm/min are shown in Figure 3(a). The spectra of the 0.1 at% Ce-doped sample is almost the same as that of Ce:YAG single crystal, and that of the 0.5 at% Ce-doped sample shows an approximately 10 nm red shift from that of Ce:YAG single crystal attributed to self absorption. The spectra of the other grown samples show the same behavior as a function of the Ce content irrespective of the growth rate. Figure 3(b) shows the fluorescence intensity at RT. The highest intensity is observed for the 0.1 at% Ce-doped sample grown at 3 mm/min. Its temperature dependence was also measured and compared with that of the 0.5 at% sample grown at the same rate in Figure 3(c). The performance of fluorescence intensity at high temperature for the 0.1 at% Ce-doped sample grown at 3 mm/min was better than that for the 0.5 at% sample, and the measured intensity for the 0.1 at% sample at 200 °C decreases only ~8 % in comparison with that at RT. This result is comparable to or better than the performance of recently developed Ce:YAG transparent ceramics [8].

Table 2: Bulk Ce contents for $(Ce_xY_{1-x})_3Al_5O_{12}/Al_2O_3$ MGC samples and the corresponding Ce contents assuming all Ce was only in YAG phase.

Growth rate		1 mm/min	3 mm/min	5 mm/min
$x = 0.1$ (at%)	Bulk Ce content	0.043 wt%	0.042 wt%	–
	Ce in YAG	0.07 at%	0.07 at%	–
	Distribution coefficient	0.7	0.7	–
$x = 0.5$ (at%)	Bulk Ce content	0.175 wt%	0.168 wt%	0.162 wt%
	Ce in YAG	0.29 at%	0.28 at%	0.27 at%
	Distribution coefficient	0.58	0.56	0.54
$x = 1.0$ (at%)	Bulk Ce content	0.328 wt%	0.336 wt%	0.344 wt%
	Ce in YAG	0.54 at%	0.56 at%	0.57 at%
	Distribution coefficient	0.54	0.56	0.57

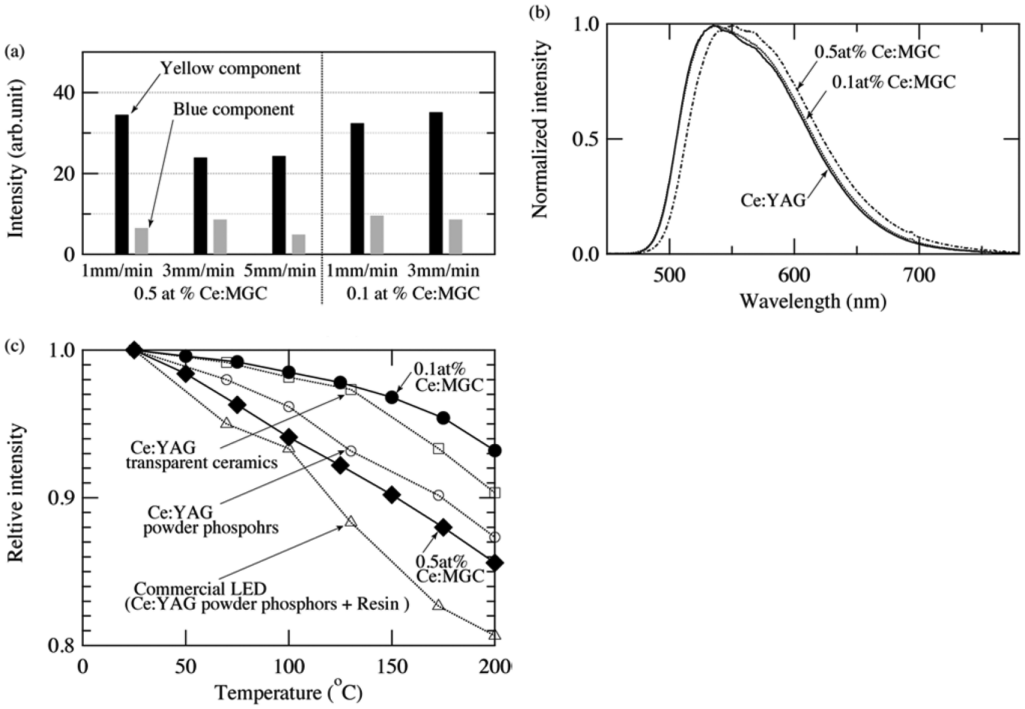

Figure 3: (a) Intensity of fluorescence: Black and gray bars indicate the intensity of yellow and blue components, respectively. (b) Normalized fluorescence spectra excited by 445 nm light: Dot-line, dot-dash line, and solid-line indicate the spectra of the 0.1 at% Ce:MGC with 3 mm/min, the 0.5 at% Ce:MGC with 3 mm/min, and Ce:YAG single crystal, respectively. (c) Temperature dependence of fluorescence intensity: Solid circles and solid diamonds indicate the intensity of the 0.1 at%Ce:MGC with 3 mm/min and the 0.5 at%Ce:MGC with 3 mm/min, respectively. Open squares, open circles, and open triangles show the literature data [8] for Ce:YAG transparent ceramics, Ce:YAG powders, and commercial LED, respectively.

Concluding remarks

Ce-doped YAG/Al_2O_3 melt-growth composites (MGCs) grown by the μ-PD method were investigated. The present MGC samples exhibit yellow fluorescence centered at 550 nm converted from 445 nm blue light, which is red shifted compared to the fluorescence from Ce:YAG single crystals. The MGC showed superior fluorescence properties without high-temperature intensity deterioration. YAG/Al_2O_3 MGC grown by μ-PD is not only a superior structural material at high temperature but is a promising material for high-power white-LED application when excited by blue LED/LD as shown in this study. From the viewpoint of producing MGC with very fine-grained texture and a higher Ce distribution coefficient, the μ-PD method is a useful and favorable method for the production of yellow phosphors for white LEDs.

Acknowledgements: We thank Mr. Shiraishi (Fukuda X'tal Lab.) for the growth by micro-pulling-down method and Mr. Narita (IMR, Tohoku Univ.) for supporting the operation of SEM, WDS, and EBSD. We also thank the Analytical Research Core for Advanced Materials (IMR, Tohoku Univ.) for the measurement of ICP-MS.

References

[1] J. Llorca and V.M. Orera, Prog. Mat. Sci., 51 (2006) 711–809.
[2] Y. Waku, H. Ohtsubo, N. Nakagawa and Y. Kohtoku, J. Mater. Sci., 31 (1996) 4663–4670.
[3] M. Yoshimura, S. Sakata, H. Iba, T. Kawano and K. Hoshikawa, J. Cryst. Growth, 416 (2015) 100–105.
[4] T. Fukuda, P. Rudolph and S. Uda, Fiber Crystal Growth from the Melt, 1st ed., Springer-Verlag, Berlin Heidelberg (2004).
[5] R. Simura, V.V. Kochurikhin, A. Yoshikawa and S. Uda, J. Cryst. Growth, 310 (2008) 2148–2151.
[6] C.A. Schneider, W.S. Rasband and K.W. Eliceiri, Nature Methods, 9 (2012) 671–675.
[7] R. Simura, A. Yoshikawa and S. Uda, J. Cryst. Growth, 311 (2009) 4763–4769.
[8] G.H. Liu, Z.Z. Zhou, Y. Shi, Q. Liu, J.Q. Wan and Y.B. Pan, Mater. Lett., 139 (2015) 480–482.